

# Different multi-fractal behaviors of diurnal temperature range over the north and the south of China

Naiming Yuan · Zuntao Fu · Jiangyu Mao

Received: 18 June 2012 / Accepted: 31 August 2012 / Published online: 16 September 2012  
© Springer-Verlag 2012

**Abstract** Multi-fractal behaviors of diurnal temperature range (DTR for short) from 100 stations over China during 1956–2010 are analyzed by means of multi-fractal detrended fluctuation analysis. By making a Monte-Carlo simulation, we obtain two criterions which can be used to decide whether a DTR series is significantly multi-fractal or not. With these criterions, different multi-fractal behaviors are found over the north and the south of China, and Yangtze River is roughly the dividing line. Over the north region, nearly all the considered DTR series do not show multi-fractal behaviors, while the results are completely the opposite over the south. The findings are confirmed by the scaling behaviors of the corresponding DTR magnitude series and indicate that more scale-dependent structure differences may be hidden in DTR series over the north and the south of China. Therefore, an extensive analysis of the multi-fractal behaviors are essential for a better understanding of the complex structures of the climate changes.

## 1 Introduction

It has been recognized that long-term persistence (or fractal behaviors) are ubiquitous in nature. Such as in

climate system, due to the complex interactions occurring on the land surface, ocean, and cryosphere, climate processes usually exhibit long-term persistence, which can be characterized by a Hurst exponent  $H > 1/2$  [measured by the rescaled range (R/S) analysis] (Hurst 1951; Koscielny-Bunde et al. 1998; Peng et al. 1994, 1995). In this case, the autocorrelation function  $C(s)$ , where  $s$  is lag time, decays as  $C(s) \sim s^{-\gamma}$ ,  $0 < \gamma < 1$ , with the mean correlation time  $s_{\times} = \frac{1}{C(0)} \int_0^{\infty} C(s) ds$  diverges (Kantelhardt et al. 2001; Koscielny-Bunde et al. 1998). In the power spectral analysis, this long-term persistence can also be characterized by a power law,  $S(f) \sim f^{-\beta}$ , where  $S(f) = |x(f)|^2$  is the power spectral density, and  $\{x(f)\}$ ,  $f = 0, \dots, N/2$ , is the Fourier transform of the records  $\{x_i\}$  (Talkner and Weber 2000; Weber and Talkner 2001). According to Koscielny-Bunde et al. (1998), Talkner and Weber (2000), and Weber and Talkner (2001), it has been proved that  $\beta = 1 - \gamma = 2H - 1$ . For stationary long-term persistent processes where  $1/2 < H < 1$ , one can find  $0 < \beta < 1$ , which means the long-term persistence process is between the white noise ( $\beta = 0$ ) and the  $1/f$  noise process ( $\beta = 1$ ). One calls this long-term persistent processes as “pink noise.” However, in the climate research, the (conventional) methods mentioned above may fail when trends are present in the system (such as the warming trend in temperature records). Normally, an increasing trend may lead to an overestimation of the Hurst exponent  $H$  and thus to an underestimation of  $\gamma$  (Kantelhardt et al. 2001; Koscielny-Bunde et al. 1998, 2006). It is even possible that, under the influence of a trend, uncorrelated data may be mistaken as long-term correlated ones by using the (conventional) methods. In the past two decades, several methods such as

---

N. Yuan · Z. Fu (✉)  
Laboratory for Climate and Ocean-Atmosphere Studies,  
Department of Atmospheric and Oceanic Sciences,  
School of Physics, Peking University, Beijing 100871, China  
e-mail: fuzt@pku.edu.cn

J. Mao  
LASG, Institute of Atmospheric Physics, CAS, Beijing,  
100029, China

wavelet techniques (WT) (Koscielny-Bunde et al. 1998) and detrended fluctuation analysis (DFA) (Eichner et al. 2003; Kantelhardt et al. 2001; Peng et al. 1994) have been developed and widely used due to their robustness to trends (Chen et al. 2007; Eichner et al. 2003; Fraedrich and Blender 2003; Király et al. 2006; Király and Jánosi 2005; Lennartz and Bunde 2009, 2011; Malamud and Turcotte 1999; Monetti et al. 2003; Rybski et al. 2006, 2008; Weber and Talkner 2001; Yuan et al. 2010). In DFA, one considers the cumulated sum (“profile”)  $Y_i = \sum_{j=1}^i x_j$  of the record of interest  $\{x_j\}$ . After eliminating the polynomial trend in segments of length  $s$  of the profile, one can determine the dependence of the mean fluctuation function  $F(s)$  on  $s$ . For the case of long-term correlations,  $F(s)$  increases by a power law,  $F(s) \sim s^\alpha$ ,  $\alpha = 1 - \gamma/2$ , where  $\alpha > 1/2$ , and is consistent with  $H$  in mono-fractal series. However, the above-mentioned detrending approaches are still not sufficient to fully characterize the complex dynamics of climate systems. Sometimes infinite exponents are needed to depict the different scaling behaviors from large fluctuations to small fluctuations (Kantelhardt et al. 2002). Such as in the spectral analysis, two time series that have the same power spectral density can still show different scaling behaviors between large and small fluctuations since the phases in  $\{x(f)\}$  may induce nonlinear properties in the original data  $\{x_i\}$  (Ashkenazy et al. 2001, 2003; Govindan et al. 2007). This indicates a multi-fractal behavior, which is independent of the mono-fractal (or two-point linear long-term persistence) but is associated with the nonlinear properties (Barabasi and Vicsek 1991; Ivanov et al. 1999, 2001; Kantelhardt 2008; Schmitt et al. 1995). It has been pointed out that to study the long-term persistence of a climate process is essential and important for the climate model evaluation and the improvement of the understanding on the climate system (Blender and Fraedrich 2003; Bunde et al. 2001; Fraedrich and Blender 2003; Govindan et al. 2002; Vyushin et al. 2004). In this article, we mainly focus on the multi-fractal (nonlinear) properties of the diurnal temperature range (DTR) over China in the last 50 years.

Diurnal temperature range, which is defined as the difference between daily maximum and daily minimum temperatures, is an important meteorological variable. It has been recognized in the meteorological community that, due to the asymmetric increasing trend of the minimum and maximum temperatures, there is a decreasing trend of DTR in the last few decades over most regions of the world (Easterling et al. 1997; Liu et al. 2004). Besides the decreasing trend, many other

properties have also been found during the last few years, such as the weekend effect (Forster and Solomon 2003; Gong et al. 2006) and the long-term correlations (Yuan et al. 2010). In an earlier work (Yuan et al. 2010), we have employed DFA to determine the scaling behaviors of DTR for the last 50 years over China. We found that the DFA exponent  $\alpha$  are above 0.5 and around 0.64. Although  $\alpha$  varies over different regions of China, the range for DFA exponent  $\alpha$  is relatively smaller than that of the mean, minimum, and maximum temperature. This suggests that remarkable geographical dependence may not exist if only two-point long-term correlations are considered. However, as we mentioned above, two time series with the same long-term correlations may still show different multi-fractal behaviors, which is related to the nonlinear properties. In this article, we employ a multi-fractal generalization of the detrended fluctuation analysis (MF-DFA), which has been widely used lately (Bogachev et al. 2007; Feng et al. 2009; Kantelhardt et al. 2006; Koscielny-Bunde et al. 2006; Telesca et al. 2005) to the DTR records during the last 55 years (1956–2010) over China to see if the multi-fractal property of DTR has a remarkable geographical dependence. We would like to note that, other methods, such as the well-developed wavelet-transform modulus maxima method, can also be used to characterize the multi-fractal behaviors, and the accuracy of both methods are equivalent (Kantelhardt et al. 2002; Muzy et al. 1993; Oświecimka et al. 2006). In our analysis, we apply MF-DFA but do not use approaches or models as mentioned in Koscielny-Bunde et al. (2006) and Kantelhardt et al. (2006), to estimate the singularity spectrums. Instead, by using Monte-Carlo simulations, we obtain two criteria which can be used to decide whether a DTR time series is significantly multi-fractal or not (for more details, see Section 2). In the end, we further confirm our findings by analyzing the fractal properties of the corresponding DTR magnitude series, which is derived from the original DTR series and has been considered as a good indicator of the nonlinearity of original data (Kalisky et al. 2005; Lu et al. 2012).

The rest of the paper is organized as follows. In Section 2, we will make a short introduction of the data sets and describe the method MF-DFA, as well as the Monte-Carlo simulation we made. Results, including the distribution of stations with different multi-fractal behaviors and scaling behaviors of the corresponding magnitude series are provided in Section 3. In Section 4, discussions and conclusions are made.

## 2 Data and methodology

### 2.1 Data sets

In this article, daily minimum and maximum temperature (which is used to determine the diurnal temperature range) from 100 stations are used for our analysis. The data are obtained from the China Meteorological Data Sharing Service System (<http://cdc.cma.gov.cn>), with length of 55 years, from 1956 to 2010. All the 100 meteorological stations are taking part in international exchange, and the data have been homogenized (Li et al. 2009). Since the length of the records is about 20,000 days, the scaling range we analyze is mainly from 100 to 1,000 days.

Before our analysis, we first eliminate the periodic seasonal trend by (a) subtracting the seasonal cycle  $T_i - \langle T_i \rangle$ , where  $T_i$  is the considered DTR, and  $\langle T_i \rangle$  is the mean DTR averaged from each calendar data, and (b) dividing  $T_i - \langle T_i \rangle$  by the standard deviation for each calendar date, as that of Kantelhardt et al. (2006),

$$\tau_i = \frac{T_i - \langle T_i \rangle}{\langle (T_i - \langle T_i \rangle)^2 \rangle^{1/2}} \tag{1}$$

where  $\tau_i$  is the standardized record, which is used for our multi-fractal analysis.

### 2.2 Methodology outline

#### 2.2.1 Multi-fractal detrended fluctuation analysis

In MF-DFA (Kantelhardt et al. 2002), one considers the cumulated sum (“profile”)  $Y_k = \sum_{i=1}^k \tau_i$  of the record  $\{\tau_i\}$ . The profile series is first divided into non-overlapping segments of equal length  $s$  indexed by  $k = 1, 2, 3, \dots, N_s$ , with  $N_s = \lceil N/s \rceil$ . Since the length of the series is not always a multiple of  $s$ , as a result, there will often remain a short part left at the end of the profile. To solve this problem, the same procedure is repeated from the other end of the record and then  $2N_s$  segments are obtained altogether. Next, in each segment  $\nu$ ,  $\nu = 1, \dots, 2N_s$ , we determine the local trend by polynomial fit and calculate the standard deviation around this fit:

$$F_s^2(\nu) = \frac{1}{s} \sum_{i=1}^s \{Y[(\nu - 1)s + i] - y_\nu(i)\}^2, \tag{2}$$

where  $y_\nu(i)$  is the fitting polynomial in segment  $\nu$ . Linear, quadratic, or higher order polynomials can be used in the fitting procedure, which corresponds to MF-DFA-1, MF-DFA-2, etc. Kantelhardt et al. (2002) (In

this article, we use MF-DFA-3 for our multi-fractal analysis). Then, an averaging procedure is performed over all the segments to determine the  $q$ th order DFA fluctuation function  $F(s)$ ,

$$F(s) = \left[ \frac{1}{2N_s} \sum_{\nu=1}^{2N_s} F_s^2(\nu)^{q/2} \right]^{1/q}, \tag{3}$$

where the index variable  $q$  can take any real value. For  $q = 2$ , the standard DFA procedure is retrieved. For long-term correlated time series,  $F_q(s)$  increases as a power-law:  $F_q(s) \sim s^{H(q)}$ , where  $H(q)$  is the generalized Hurst exponent. When  $q$  is positive,  $H(q)$  describes the scaling behavior of large fluctuations, while small fluctuations determine  $H(q)$  when  $q$  is negative. For a mono-fractal time series,  $H(q)$  is independent of  $q$ , while for a multi-fractal time series,  $H(q)$  varies with  $q$ . This is the so-called multi-fractal process (Kantelhardt et al. 2002).

It is worth noting that when  $q = 0$ , we cannot determine  $H(0)$  directly by using Eq. 3. Instead, we can employ a logarithmic averaging procedure (Kantelhardt et al. 2002),

$$F_0(s) = \exp \left\{ \frac{1}{4N_s} \sum_{\nu=1}^{2N_s} \ln [F_s^2(\nu)] \right\} \sim s^{H(0)}. \tag{4}$$

To characterize the multi-fractal properties of a time series, one can link  $H(q)$  with the singularity spectrum  $D(h)$  via a Legendre transform,

$$h = H(q) + q \frac{dH(q)}{dq}, \tag{5}$$

and

$$D(h) = q(h - H(q)) + 1, \tag{6}$$

where  $h$  is the singularity strength or Hölder exponent, and  $D(h)$  denotes the dimension of the subset of the series (Kantelhardt et al. 2002; Lin and Fu 2008; Muzy et al. 1993). To calculate  $h$  and  $D(h)$  from  $H(q)$ , several methods, such as the generalized binomial multiplicative cascade model, are widely used. With these methods, one can fit the relation between  $H(q)$  and  $q$ , and further obtain the singularity spectrum  $D(h)$  and the singularity strength  $h$ . The width of the singularity spectrum  $\Delta h$  is thus obtained to characterize the strengths of multi-fractal behaviors (Feng et al. 2009; Kantelhardt et al. 2006, 2002; Koscielny-Bunde et al. 2006).

However, we would like to note that the singularity strength  $h$  (or the width of the singularity spectrum

$\Delta h$ ) obtained from the mentioned methods, such as the generalized binomial multiplicative cascade model, might be doubtful. First, since the typical length of observed daily climate records is only around  $10^4$ , we cannot make  $|q|$  too large. Normally, the range of  $q$  is selected as  $[-5, 5]$  or  $[-10, 10]$ , depending on the length of the considered record. Thus, the fit of the relation between  $H(q)$  and  $q$  based on this small  $q$  range may have problems in representing and predicting the  $H(q) \sim q$  behaviors when  $q$  is large (e.g.,  $q = 20, 50$ , or even larger). Furthermore, in MF-DFA, scaling behaviors of  $F(s)$  vs  $s$  fluctuate more tremendously for large  $|q|$ , especially when  $q$  is negative. These relatively large fluctuations due to poor statistics may lead to an unreliable measurement of  $H(q)$ , and thus may result in an uncertain fitness of  $H(q) \sim q$ . Therefore, one should be very careful when trying to characterize the strengths of multi-fractal behaviors. In our study, we do not care how strong the multi-fractal behavior is in each considered DTR series. We only ask whether the considered DTR series shows significant multi-fractal behavior (or nonlinear property) or not, and is there a remarkable geographical dependence of the stations with significant and non-significant multi-fractal behaviors.

### 2.2.2 Criterion for multi-fractal behaviors

In order to determine if a considered DTR series is significantly multi-fractal or not, two criterions,  $\Delta_\sigma$  and  $\Delta_{0.95}$ , are estimated by using Monte-Carlo simulation. According to Yuan et al. (2010), the mean DFA2

exponent for DTR series over China is  $\alpha = 0.64$ . Therefore, artificial mono-fractal data with the same exponent  $\alpha$  are generated and the length is 20,000, which is similar to the length of DTR series we analyze in our study. Our main aim is to determine when MF-DFA is applied to the mono-fractal data, the range of  $H(q)$  due to uncertainty of the computation (or the finite size effect). As Ashkenazy et al. (2001, 2003) and Govindan et al. (2007) mentioned, the multi-fractal behaviors (or the nonlinear properties) are related with the phases in  $\tau(f)$ , where  $\{\tau(f)\}$  is the Fourier transform of the records  $\{\tau_i\}$ . One can randomize the phases, but keep the power spectral density unchanged, to remove the multi-fractal behaviors (or nonlinear properties) hidden in the data. This is the so-called phase randomize surrogate procedure (PRS). In our study, we apply PRS to the artificial mono-fractal data and repeat 1,000 times to obtain 1,000 time series characterized by the same two-point correlation (or mono-fractal behavior). Due to the randomization of the phases, these 1,000 time series are all not characterized by multi-fractal behaviors. Then we apply MF-DFA to all these 1,000 time series with  $q$  ranges from  $-5$  to  $5$ . Theoretically, since the time series are all mono-fractal,  $H(q)$  should be independent of  $q$  and has the value of 0.64. However, due to the uncertainties we mentioned above, the measured  $H(q)$  may have deviations from 0.64. In this way, for each  $q$ , we have 1,000 samples to obtain a mean  $\bar{H}(q)$  and its standard deviation  $\sigma_q$  as error bars. Figure 1 shows the results. In Fig. 1a, we can see that the standard deviation  $\sigma_q$  varies for different  $q$ . Relatively higher  $\sigma_q$  can be found when  $q$  is

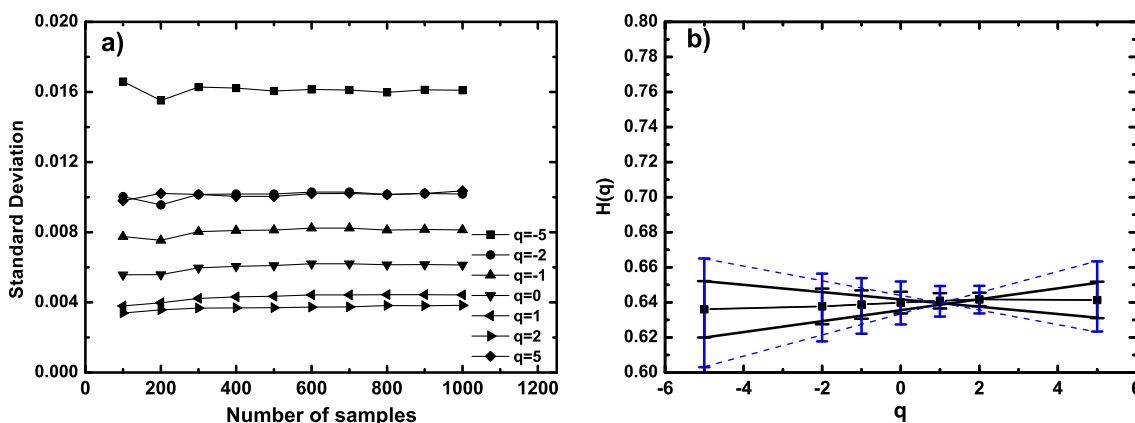


**Fig. 1** Estimation of the computation of uncertainties for  $H(q)$ . From 1,000 artificial samples, the standard deviation  $\sigma_q$  for different  $q$  is shown (a). Relatively higher  $\sigma_q$  can be found when  $q$  is negative, and  $\sigma_q$  becomes stable when the number of sample is larger than 400; the mean  $H(q)$  with error bars  $\sigma_q$  and  $R_{0.95}$  is shown b. The error bars  $\sigma_q$  are shown in black, which is used

to determine the first criterion  $\Delta_\sigma = 0.032$ . The error bars  $R_{0.95}$ , which are shown in blue, are the varying ranges of  $H(q)$  when 95 % of all the samples (2.5 % of the samples with the highest  $H(q)$  and the other 2.5 % of the samples with the lowest  $H(q)$  are excluded) are considered. With  $R_{0.95}$ , one can estimate the other criterion  $\Delta_{0.95} \approx 0.06$

negative, which may be due to the tremendous fluctuation of  $F(s)$  as we mentioned above. Meanwhile,  $\sigma_q$  also varies as a function of the sample numbers. When the number of sample reach 400,  $\sigma_q$  becomes stable. This indicates that the 1,000 time series we use is enough for our estimation. Taking  $\sigma_q$  as an error bar (black in Fig. 1b), one can estimate the range of  $H(q)$ , which may be due to the uncertainty of the computation. The range is defined as the difference between the biggest  $[H(q) + \sigma_q]$  and the smallest  $[H(q) - \sigma_q]$ . In our work, it is  $\Delta_\sigma = [H(5) + \sigma_{q=5}] - [H(-5) + \sigma_{q=-5}] = 0.032$ , where  $\Delta_\sigma$  can be used as a criterion for determining whether a considered DTR series is multi-fractal or not. Besides  $\Delta_\sigma$ , we further define another criterion  $\Delta_{0.95}$ , which can be used to determine whether the multi-fractal behavior is significant or not, within the confidence probability of 0.95. See that in Fig. 1b, the *blue* error bars  $R_{0.95}$  represent the varying range of  $H(q)$  when 95 % of all the samples (2.5 % of the samples with the highest  $H(q)$  and the other 2.5 % of the samples with the lowest  $H(q)$  are excluded) are considered. One can find  $\Delta_{0.95} \approx 0.06$  from the figure. Therefore, if the range of  $H(q)$  obtained from a DTR series is larger than  $\Delta_{0.95}$ , one can say the multi-fractal behavior is significant (within the confidence probability of 0.95). If the range of  $H(q)$  obtained from a DTR series is larger than  $\Delta_\sigma$  but smaller than  $\Delta_{0.95}$ , we suggest that one can only say the considered DTR series may be multi-fractal, but not so strong.

### 3 Results

In our study, we first employ MF-DFA to two representative stations. One is Linxi station (44N, 118E), which is located in the northeast of China, and the other one is Guangzhou station (23N, 113E), which is located in the southern of China. Linxi is in the continental monsoon climate zone, while Guangzhou is in the subtropical monsoon climate zone. Therefore, the climatic characteristics of the two places are completely different. As for the multi-fractal behaviors, we can see in Fig. 2 that  $H(q)$  in Linxi do not seem to depend on  $q$ , while a more remarkable multi-fractal behavior can be found in Guangzhou. Figure 2a, b show, in a double-logarithmic plot, the fluctuations of  $F(s)$  as a function of  $s$  for different  $q$ . The red lines are the fitness of the fluctuations. One can see more clearly, in Fig. 2c, d, that the slopes of the lines for Guangzhou varies more remarkably for different  $q$ , and the values are ranged from  $H(5) = 0.65$  to  $H(-5) = 0.72$  (see Fig. 2f). For Linxi in Fig. 2e, there seems to be no changes in  $H(q)$ . The different results for the two representative stations

suggest that there may be different multi-fractal behaviors for stations over different regions or climate zones. Therefore, we further consider 100 stations over China in order to see if there is a geographical dependence of the multi-fractal behaviors. By using the Monte-Carlo simulation described above in Section 2.2, we have determined two criterions  $\Delta_\sigma = 0.032$  and  $\Delta_{0.95} = 0.06$  (see Fig. 1b), which means if the varying range of  $H(q)$ ,  $\Delta H$ , is larger than  $\Delta_\sigma = 0.032$ , the considered DTR series may be characterized by multi-fractal. If  $\Delta H > \Delta_{0.95} = 0.06$ , the multi-fractal behavior is significant. In contrary, if  $\Delta H < \Delta_\sigma = 0.032$ , we assume there are no multi-fractal behaviors. Actually, there might be weak multi-fractal behavior, but it is too weak for us to distinguish from the cases with strong uncertainties of the computation. We apply MF-DFA to all the 100 stations and calculate the varying range for  $H(q)$ . A geographical dependence of multi-fractal behaviors is found in Fig. 3, where the open circles stand for the DTR series with  $\Delta H < \Delta_\sigma$ , which means no multi-fractal behaviors can be detected, while solid circles are stations where multi-fractal properties are found (with  $\Delta H > \Delta_\sigma$ ). Solid circles with larger size (as shown in Fig. 3) are stations where the DTR series have significant multi-fractal behaviors (with  $\Delta H > \Delta_{0.95}$ ). Interestingly, we find a remarkable difference of DTR multi-fractal behaviors over the south and the north regions of China, and Yangtze River is roughly the dividing line. In the north of Yangtze River, nearly all the considered DTR series do not have multi-fractal behaviors, while in the south of Yangtze River, the results are completely the opposite. The range of  $H(q)$  for most of the stations are larger than  $\Delta_\sigma$ , while some of them even have significant multi-fractal behaviors with  $\Delta H > \Delta_{0.95}$ . Notice that there are no obvious geographical dependence of the mono-fractal behaviors (Yuan et al. 2010); the results of the multi-fractal behaviors shown in Fig. 3 may suggest more scale-dependent and complex structure differences hidden in DTR series. Therefore, the multi-fractal analysis seems to be more important for us to understand and interpret how the climate factors affect the DTR series.

In order to confirm our findings, we further apply DFA2 to the corresponding DTR magnitude series  $|\tau_i|$ , where  $\tau_i$  are the seasonal detrended DTR records (see Eq. 1). DFA2 can be considered as a special case of MF-DFA, when  $q = 2$  and the local trend is estimated by a quadratic polynomial fit (note that in the multi-fractal analysis above, local trend in “profile”  $Y_k$  are estimated by a cubic polynomial fit (MF-DFA-3). Here, in the memory analysis of the magnitude series, quadratic detrending is enough for removing the effect of external trend and obtaining reliable results). Many works have

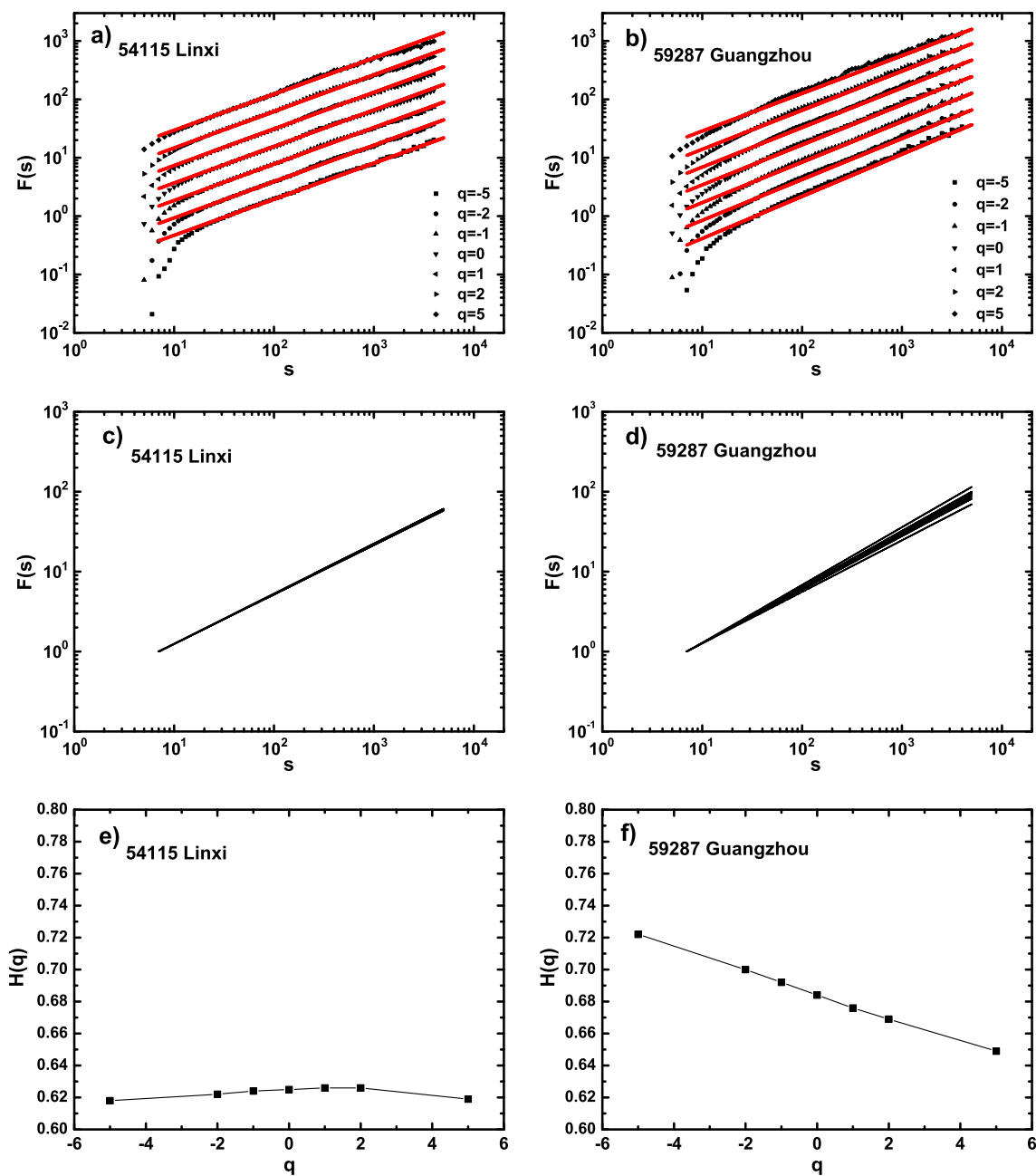


**Fig. 2** MF-DFA results for two representative stations, Linxi (left hand side) and Guangzhou (right hand side). **a, b** In a double-logarithmic plot, the fluctuation  $F(s)$  as a function of  $s$  for different  $q$  is shown. The red lines are the fitness of the slope.

**c, d** The fitness of the slope in a much clearer way. **e, f** The variation of  $H(q) \sim q$ . For different  $q$ , nearly no variation is found in Linxi, while  $H(q)$  for Guangzhou varies more obviously

shown that the multi-fractal behaviors are related to their nonlinear properties of the original data. This nonlinearity can be estimated from the fractal behaviors in the corresponding magnitude series (Ashkenazy et al. 2003; Kalisky et al. 2005; Lu et al. 2012). If the magnitude series is long-term correlated with DFA2 exponent  $\alpha > 1/2$ , we can consider the original records being characterized by nonlinear properties. In con-

trast, if the magnitude series behaves as a white noise, no pronounced nonlinear properties can be found in the original records. Since multi-fractal behaviors have close relations with this nonlinearity, to the end of this section, we put our emphasis on the analysis of the nonlinear properties, which is accessed from the scaling behaviors in magnitude series. We again take Linxi and Guangzhou as representative stations. For

**Fig. 3** Geographical dependence of multi-fractal behaviors for the DTR series over China. *Open circles* stand for the DTR series with  $\Delta H < \Delta_\sigma$ , which indicates no multi-fractal behaviors can be detected. *Solid circles* are stations where multi-fractal properties may exist ( $\Delta H > \Delta_\sigma$ ), while *solid circles with larger size* are stations where the DTR series have significant multi-fractal behaviors ( $\Delta H > \Delta_{0.95}$ ). A clear difference between the south and the north is found, with the Yangtze River roughly as the dividing line



each station, we first apply the PRS procedure to the seasonal detrended data  $\tau_i$ . As described above in Section 2.2, the nonlinearity can be eliminated when the phases are randomized, but the power spectral density (or the mono-fractal behavior) will remain unchanged. Therefore, if  $\tau_i$  is characterized by nonlinear properties, the DFA results should be different between the magnitude series  $|\tau_i|$  and the new series obtained from PRS procedure  $|\tau_i^{PRS}|$ . While for  $\tau_i$  and the data from PRS,  $\tau_i^{PRS}$ , the scaling behaviors should be the same. Figure 4 shows the results for Linxi (Fig. 4a) and Guangzhou (Fig. 4b). The squares represent the DFA results of  $\tau_i$  (solid squares) and  $\tau_i^{PRS}$  (open squares), and the circles

are the results of magnitude series (solid circles for  $|\tau_i|$ , open circles for  $|\tau_i^{PRS}|$ ). For Linxi, there are no changes of the DFA results after the PRS procedure, for both  $\tau_i$  and magnitude series  $|\tau_i|$ . Actually, the DFA exponent  $\alpha$  obtained from the magnitude series are  $\alpha \approx 0.5$ , which indicates a white noise behavior. This means that the DTR series observed in Linxi does not have pronounced nonlinear properties, which is consistent with our findings in Fig. 2. While for Guangzhou, although, as expected, no changes are found in the DFA results for  $\tau_i$  and  $\tau_i^{PRS}$ , significant deviations of the DFA curves, however, arise for the magnitude series. Before the PRS procedure, the magnitude series  $|\tau_i|$

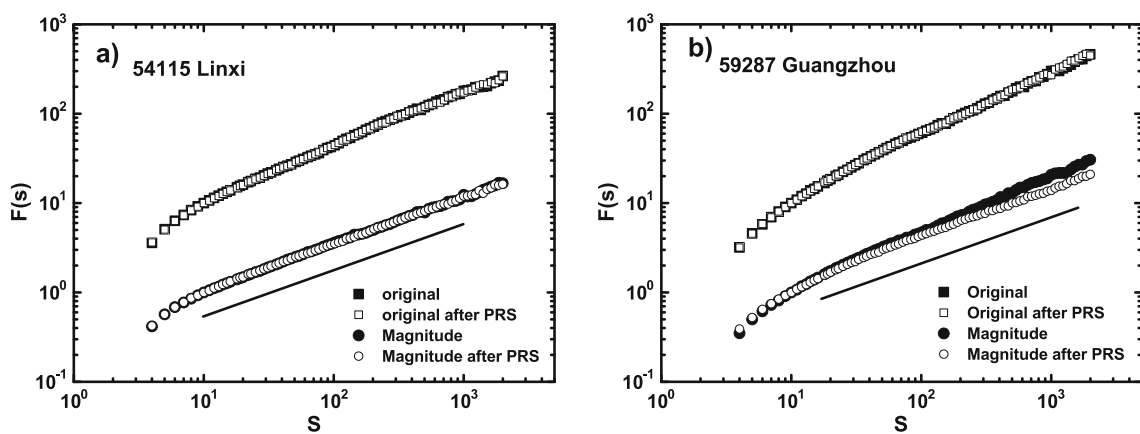


**Fig. 4** DFA2 results for the seasonal detrended DTR  $\{\tau_i\}$ , the data after the phase randomize surrogate procedure (PRS)  $\{\tau_i^{PRS}\}$ , and the corresponding magnitude series  $\{|\tau_i|\}$ ,  $\{|\tau_i^{PRS}|\}$ . *Squares* represent the DFA results of original data: (*solid square* for  $\{\tau_i\}$  and *open squares* for  $\{\tau_i^{PRS}\}$ ); and *circles* are the results of magnitude series: (*solid circles* for  $\{|\tau_i|\}$  and *open circles* for

$\{|\tau_i^{PRS}|\}$ ). **a** Results of Linxi, where no changes of the DFA results are found after the PRS procedure for both the  $\{\tau_i\}$ ,  $\{\tau_i^{PRS}\}$  and magnitude series  $\{|\tau_i|\}$ ,  $\{|\tau_i^{PRS}|\}$ . **b** Results of Guangzhou, after the PRS procedure, where we can see clear deviations in the DFA curves for the magnitude series. The *black line* in both figures have a slope of 0.5

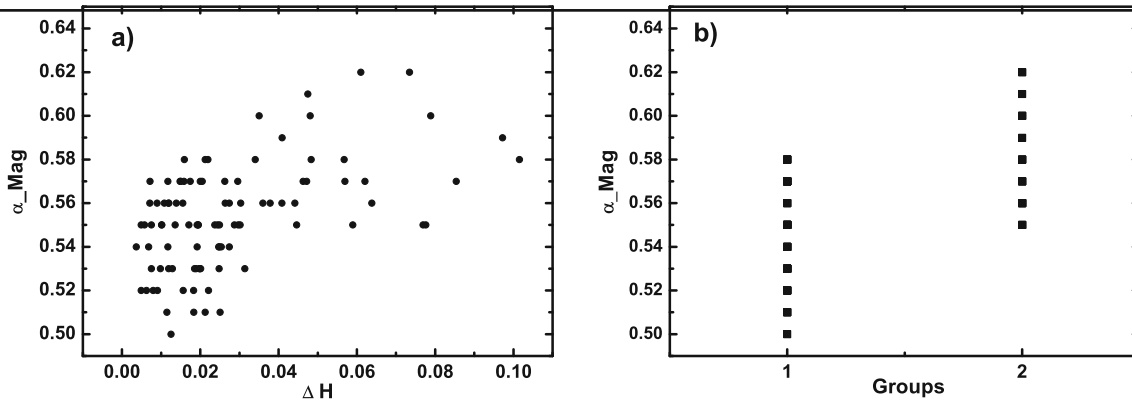


**Fig. 5** DFA2 exponent  $\alpha_{Mag}$  of magnitude series  $\{|\tau_i|\}$  obtained from all the considered 100 stations. **a** Relations between  $\alpha_{Mag}$  and the varying range of  $H(q)$ ,  $\Delta H$ . One can see that stations with higher  $\Delta H$  have bigger chances to have higher  $\alpha_{Mag}$ . **b** All the stations are divided into two groups according to Fig. 3. Sta-

tions which do not have multi-fractal behaviors ( $\Delta H < \Delta_\sigma$ ) are in group 1, while the other stations with multi-fractal behaviors ( $\Delta H > \Delta_\sigma$ ) in group 2. One can find relatively higher DFA2 exponents  $\alpha_{Mag}$  in Group-2

has a DFA exponent of  $\alpha = 0.62$ , but after the PRS procedure, the DFA exponent becomes much smaller, with  $\alpha \approx 0.5$ . According to Kalisky et al. (2005) and Lu et al. (2012), this result indicates a pronounced nonlinearity behavior in the DTR series observed in Guangzhou, which again keeps in line with our findings in Fig. 2. By comparing Fig. 4 with Fig. 2, we could also suggest that the scaling behaviors of magnitude series is a good indicator of the nonlinearity or the multi-fractal property of a considered original time series. We further consider the scaling behaviors of magnitude series obtained from all the 100 stations. Figure 5a shows the relations between the DFA exponents of the magnitude series  $\alpha_{Mag}$  and the corresponding  $\Delta H$  obtained above. One can easily find that for higher  $\Delta H$ , the  $\alpha_{Mag}$  have a big chance to become also higher. If we classify all the stations into two groups according to Fig. 3, where stations without multi-fractal behaviors ( $\Delta H < \Delta_\sigma$ ) are in group 1 (75 stations) and stations with multi-fractal behaviors ( $\Delta H > \Delta_\sigma$ ) are in group 2 (25 stations), we can see the DFA exponents are relatively higher in group 2 than that in group 1 (see Fig. 5b). By comparing with Fig. 3, the results suggest that the scaling behaviors of magnitude series are indeed a good indicator of the nonlinear properties (or multi-fractal behaviors) of the considered data  $\tau$ . Furthermore, based on these two figures, one can believe that the multi-fractal behaviors (or the nonlinear properties) of DTR are indeed different over the north and the south of China.

#### 4 Discussion and conclusion

It is not surprising that there are significant differences of the climate conditions over the north and the south

of China. Factors like the latitude, continent–ocean locations, and the terrain conditions, etc. are all different and can further result in different characteristics of the climate change. As in the south, climate processes may be more affected by multi-scale processes than that in the north due to the influence of the tropical convective activities, monsoon, the effect of Qinghai-Tibet Plateau, and even the ENSO happens in the Pacific, etc. Wu and Zhang (1998), Wang et al. (2008, 2000), Wu et al. (2007). All these strong factors may be responsible for the nonlinearities in the climatic variabilities over the south of China.

Since the nonlinear properties might be more significant in the south of China than that in the north, one may directly wonder if we can find some hints of the nonlinearities from the original series. Figure 6 shows the DTR series obtained from Linxi (one station from the north of China) and Guangzhou (one station from the south of China). One can find that the fluctuations in Linxi are relatively more uniform, while more cluster structures arose in Fig. 6b (for Guangzhou). This cluster structure might be one manifestation of the nonlinear properties, and a multi-fractal analysis may be useful for our understanding of the nonlinear properties.

In this article, we employ the MF-DFA to the DTR of the past 55 years over China. Interestingly, different multi-fractal behaviors of DTR are found over the south and the north of China, and the Yangtze River is roughly the dividing line. In the north of Yangtze River, nearly all the considered DTR series do not show multi-fractal behaviors (with  $\Delta H < \Delta_\sigma$ ), while in south of Yangtze River, the results are completely the opposite. By further analyzing the fractal behaviors of the magnitude series  $|\tau_i|$  by means of DFA2, we find that the DTR series observed from south of Yangtze

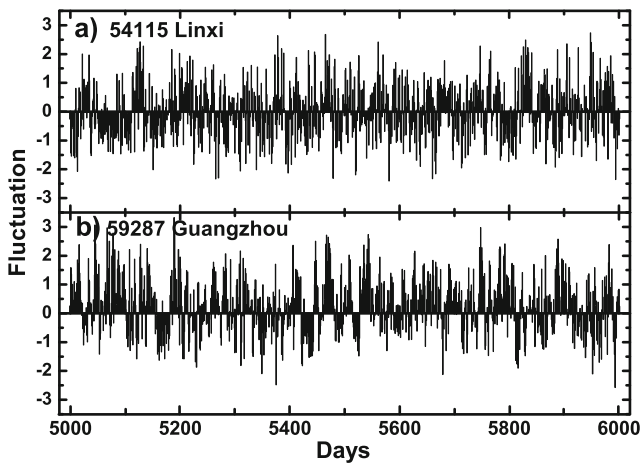


**Fig. 6** Segments of the DTR series  $\{\tau_i\}$ . **a** Linxi. **b** Guangzhou. One can find that the fluctuations in Linxi are relatively more uniform, while more cluster structures arose in the series of Guangzhou

River do show significant nonlinear properties, which indicates a close relationship between the nonlinear property and the multi-fractal behavior. Therefore, the multi-fractal behaviors, which can be determined from MF-DFA easily, could be considered as a good manifestation of the nonlinear properties. Through multi-fractal analysis, one can get more information from the climate processes than in cases when only mono-fractal analysis are made. Thus, for better understanding of the complex structures of climate change or better evaluations of the climate models, multi-fractal analysis is essential and important.

**Acknowledgements** Many thanks are due to supports from the National Natural Science Foundation of China (nos. 41175141 and 41175059) and from the National Basic Research Programme of China (no. 2011CB403505).

## References

- Ashkenazy Y, Ivanov PC, Havlin S, Peng C-K, Goldberger AL, Stanley HE (2001) Magnitude and sign correlations in heartbeat fluctuations. *Phys Rev Lett* 86:1900
- Ashkenazy Y, Havlin S, Ivanov PC, Peng C-K, Schulte-Frohlinde V, Stanley HE (2003) Magnitude and sign scaling in power-law correlated time series. *Physica, A* 323:19
- Barabasi AL, Vicsek T (1991) Multifractality of self-affine fractals. *Phys Rev A* 44:2730
- Blender R, Fraedrich K (2003) Long time memory in global warming simulations. *Geophys Res Lett* 30:1769
- Bogachev MI, Eichner JF, Bunde A (2007) Effect of nonlinear correlations on the statistics of return intervals in multifractal data sets. *Phys Rev Lett* 99:240601
- Bunde A, Havlin S, Koscielny-Bunde E, Schellnhuber H-J (2001) Long term persistence in the atmosphere: global laws and tests of climate models. *Physica, A* 302:255

- Chen X, Lin G, Fu Z (2007) Long-range correlations in daily relative humidity fluctuations: a new index to characterize the climate regions over China. *Geophys Res Lett* 34: L07804
- Easterling DR, Horton B, Jones PD, Peterson TC, Karl TR, Parker DE, Salinger MJ, Razuvayev V, Plummer N, Jamason P, Folland CK (1997) Maximum and minimum temperature trends for the globe. *Science* 277: 364
- Eichner JF, Koscielny-Bunde E, Bunde A, Havlin S, Schellnhuber H-J (2003) Power-law persistence and trends in the atmosphere: a detailed study of long temperature records. *Phys Rev E* 68:046133
- Feng T, Fu Z, Deng X, Mao J (2009) A brief description to different multi-fractal behaviors of daily wind speed records over China. *Phys Lett A* 373:4134
- Forster PM, Solomon S (2003) Observations of a “weekend effect” in diurnal temperature range. *Proc Natl Acad Sci* 100:11225
- Fraedrich K, Blender R (2003) Scaling of atmosphere and ocean temperature correlations in observations and climate models. *Phys Rev Lett* 90:108501
- Gong D, Guo D, Ho CH (2006) Weekend effect in diurnal temperature range in China: opposite signals between winter and summer. *J Geophys Res* 111:D18113
- Govindan RB, Vyushin D, Bunde A, Brenner S, Havlin S, Schellnhuber H-J (2002) Global climate models violate scaling of the observed atmospheric variability. *Phys Rev Lett* 89:028501
- Govindan RB, Wilson JD, Preißl H, Eswaran H, Campbell JQ, Lowery CL (2007) Detrended fluctuation analysis of short datasets: an application to fetal cardiac data. *Physica, D* 226:23
- Hurst HE (1951) Long-term storage capacity of reservoirs. *Trans Am Soc Civ Eng* 116:770
- Ivanov PC, Amaral LAN, Goldberger AL, Havlin S, Rosenblum MG, Struzik ZR, Stanley HE (1999) Multifractality in human heartbeat dynamics. *Nature* 399:461
- Ivanov PC, Amaral LAN, Goldberger AL, Havlin S, Rosenblum MG, Stanley HE, Struzik ZR (2001) From 1/f noise to multifractal cascades in heartbeat dynamics. *Chaos* 11:641
- Kalisky T, Ashkenazy Y, Havlin S (2005) Volatility of linear and nonlinear time series. *Phys Rev E* 72:011913
- Kantelhardt JW (2008) Fractal and multifractal time series. In: Springer encyclopaedia of complexity and system science. [arXiv: 0804.0747v1](https://arxiv.org/abs/0804.0747v1) [physics.data-an]
- Kantelhardt JW, Koscielny-Bunde E, Rego HHA, Havlin S (2001) Detecting long-range correlations with detrended fluctuation analysis. *Physica, A* 295:441
- Kantelhardt JW, Koscielny-Bunde E, Rybski D, Braun P, Bunde A, Havlin S (2006) Long-term persistence and multifractality of precipitation and river runoff records. *J Geophys Res* 111:D01106
- Kantelhardt JW, Zschiegner SA, Koscielny-Bunde E, Havlin S, Bunde A, Stanley HE (2002) Multifractal detrended fluctuation analysis of nonstationary time series. *Physica, A* 316:87
- Király A, Bartos I, Jánosi IM (2006) Correlation properties of daily temperature anomalies over land. *Tellus* 58A:593
- Király A, Jánosi IM (2005) Detrended fluctuation analysis of daily temperature records: geographic dependence over Australia. *Meteorol Atmos Phys* 88:119
- Koscielny-Bunde E, Bunde A, Havlin S, Roman HE, Goldreich Y, Schellnhuber H-J (1998) Indication of a

- universal persistence law governing atmospheric variability. *Phys Rev Lett* 81:729
- Koscielny-Bunde E, Kantelhardt JW, Braun P, Bunde A, Havlin S (2006) Long-term persistence and multifractality of river runoff records: detrended fluctuation studies. *J Hydrol* 322:120
- Lennartz S, Bunde A (2009) Trend evaluation in records with long-term memory: application to global warming. *Geophys Res Lett* 36:L16706
- Lennartz S, Bunde A (2011) Distribution of natural trends in long-term correlated records: a scaling approach. *Phys Rev E* 84:021129
- Li Q, Zhang H, Chen J, Li W, Liu X, Jones P (2009) A mainland China homogenized historical temperature dataset for 1951–2004. *Bull. Amer. Meteor. Soc* 90:1062
- Lin G, Fu Z (2008) A universal model to characterize different multi-fractal behaviors of daily temperature records over China. *Physica, A* 387(2008):573
- Liu B, Xu M, Henderson M, Qi Y, Li Y (2004) Taking China's temperature: daily range, warming trends, and regional variations, 1955–2000. *J Climate* 17:4453
- Lu F, Yuan N, Fu Z, Mao J (2012) Universal scaling behaviors of meteorological variables' volatility and relations with original records. *Physica, A*. doi:10.1016/j.physa.2012.05.031
- Malamud BD, Turcotte DL (1999) Long term persistence in geosciences. *Adv Geophys* 40:1
- Monetti RA, Havlin S, Bunde A (2003) Long term persistence in the sea surface temperature fluctuations. *Physica, A* 320:581
- Muzy JF, Bacry E, Arneodo A (1993) Multifractal formalism for fractal signals: the structure-function approach versus the wavelet-transform modulus-maxima method. *Phys Rev E* 47:875
- Oświecimka P, Kwapień J, Drożdż S (2006) Wavelet versus detrended fluctuation analysis of multifractal structures. *Phys Rev E* 74:016103
- Peng CK, Buldyrev SV, Havlin S, Simons M, Stanley HE, Goldberger AL (1994) Mosaic organization of DNA nucleotides. *Phys Rev E* 49:1685
- Peng CK, Havlin S, Stanley HE, Goldberger AL (1995) Quantification of scaling exponents and crossover phenomena in nonstationary heartbeat time series. *Chaos* 5:82
- Rybski D, Bunde A, Havlin S, von Storch H (2006) Long-term persistence in climate and the detection problem. *Geophys Res Lett* 33:L06718
- Rybski D, Bunde A, von Storch H (2008) Long-term memory in 1000-year simulated temperature records. *J Geophys Res* 113:D02106
- Schmitt F, Lovejoy S, Schertzer D (1995) Multifractal analysis of the Greenland ice-core project climate data. *Geophys Res Lett* 22:1689
- Talkner P, Weber RO (2000) Power spectrum and detrended fluctuation analysis: application to daily temperature. *Phys Rev E* 62:150
- Telesca L, Lapenna V, Macchiato M (2005) Multifractal fluctuations in seismic interspike series. *Physica, A* 354:629
- Vyushin D, Zhidkov I, Havlin S, Bunde A, Brenner S (2004) Volcanic forcing improves atmosphere-ocean coupled general circulation model scaling performance. *Geophys Res Lett* 31:L10206
- Wang B, Bao Q, Hoskins B, Wu G, Liu Y (2008) Tibetan Plateau warming and precipitation changes in East Asia. *Geophys Res Lett* 35:L14702
- Wang B, Wu R, Fu X (2000) Pacific–East Asian teleconnection: How does ENSO affect East Asian climate?. *J Climate* 13:1517
- Weber RO, Talkner P (2001) Spectra and correlations of climate data from days to decades. *J Geophys Res* 106:20131
- Wu G, Liu Y, Wang T, Wan R, Liu X, Li W, Wang Z, Zhang Q, Duan A, Liang X (2007) The influence of mechanical and thermal forcing by the Tibetan Plateau on Asian climate. *J Hydrometeorol* 8:770
- Wu G, Zhang Y (1998) Tibetan Plateau forcing and the timing of the monsoon onset over South Asia and the South China Sea. *Mon Weather Rev* 126:913
- Yuan N, Fu Z, Mao J (2010) Different scaling behaviors in daily temperature records over China. *Physica, A* 389:4087